

Steep-edge filter design with equivalent layers

Uwe B. Schallenberg

mso jena Mikroschichtoptik GmbH, Carl-Zeiss-Promenade 10, D-07745 Jena, Germany
u.schallenberg@mso-jena.de

ABSTRACT

Based on a special definition of the edge region of a thin-film interference filter, an approach to design steep-edge filters using the theory of equivalent layers is presented. Some features are discussed using the known theory to meet the topical filter requirements. An example is theoretically outlined and the spectral performance of a manufactured filter is presented.

Keywords: thin-film optical filters, equivalent layers, edge filters

1. INTRODUCTION

Thin-film edge filters as long-wave passes or short-wave passes are often essential components of an optical device. A typical application of such an edge filter is the optical arrangement used for fluorescence microscopy. In this case, a conventional microscope is supplemented at least by an excitation source, a dichroic mirror, and two edge filters as excitation filter and emission filter. State-of-the-art fluorescence detection requires steep-edges filters with spectral slopes of only few nanometers for the transition region from blocking to the pass. In this case, blocking means an optical density (OD) of OD5 in comparison with the transmission of the pass. Such a slope is in extreme contrast to the conventional definition of the slope of an edge filter which defines the distance of the wavelengths where the transmission is 5 % and 80 %.¹ Because the slope of the spectral edge of any interference filter depends directly on the number of layers, edge filters of the past were multilayers consisting of 20 to 40 layers, and state-of-the-art edge filters usually require 80 to 100 or even more layers.

This level of the number of layers of an edge filter confronts the thin-film designer with the problem of smoothing the transmission within the passband, particularly close to the edge. Normally, a problem like this can be quickly solved using a suitable optimization procedure implemented in most of the thin-film design softwares.² However, edge filter designing is also particularly connected with the theory of equivalent layers.³⁻⁶ Because this theory is an outstanding tool to generally discuss thin-film design problems and their suitable solutions, it is suggested by itself that equivalent layers are used to design steep-edge filters theoretically or to get at least a suitable design for the further refinement procedure.

The next section outlines some basics of the theory of equivalent layers in connection with a special definition of the edge region concerning the spectral performance of an edge filter. Section 3 provides an example of the derivation of a steep-edge long-wave pass filter using exclusively equivalent layers.

2. EQUIVALENT LAYERS AND EDGE REGION

Let us assume a multilayer with alternating A and B layers having different refractive indices n_A and n_B , respectively. Let us also assume that all the refractive indices are constant over the wavelength and the layers are free of any losses. The angle of incidence to the substrate surface on which the layers are deposited is normal. The reflectivity of the uncoated back surface of the substrate is ignored. All the layers are of equal optical thickness except the first layer and the last one which are of half the optical thickness as the others. A multilayer like this can be described using quarter-wave optical thickness (QWOT) by a periodical trilayer as

$$A/2 B A \dots A B A/2 \quad \text{or} \quad B/2 A B \dots B A B/2 \Rightarrow (A/2 B A/2)^p \quad \text{or} \quad (B/2 A B/2)^p$$

where the different trilayer types A/2 B A/2 and B/2 A B/2 characterize the design as long-wave pass and short-wave pass under the condition that $n_A > n_B$. The exponent p stands for p periods of the trilayer noticed in brackets.

The assumed multilayers have symmetrical layer sequences, i.e. the sequences are the same listed in reverse order of the layers. In this case, the multilayer can be mathematically described similar to the performance of a single real layer by an equivalent layer having an equivalent refractive index E , the so-called Herpin Index, and an equivalent phase thickness Γ . E and Γ are complex numbers depending on the values of the refractive indices and the wavelength. Per definition, there is a stopband if E is imaginary and a passband if E is real.⁶

The relative width of the stopband of the assumed multilayer, the transmission at the edges of the stopband, and also the minimum of transmission within the stopband depend only on the refractive indices of the materials used and the given number of the periods. Figure 1 shows the stopband transmission of an example of a long-wave pass filter, as $(A/2 B A/2)^{20}$ with $n_A = 2.35$ and $n_B = 1.47$. Related to the parameters of an edge filter, there are some characteristic points within the stopband. There is a stopband center with T_{\min} at λ_0 ; there are the spectral edges of the desired blocking region with T_{Stop} at λ_{S1} and λ_{S2} ; and there are the spectral edges of the stopband with T_{edge} at λ_{E1} and λ_{E2} . In any case, the edge filter design has to fulfil $T_{\min} < T_{\text{Stop}}$, but in the case of steep-edges there is usually $T_{\text{Stop}} < T_{\text{edge}}$. That means that the spectral edges of the stopband are not part of the blocking region, in general.

The transmission within the passband T_{Pass} is directly determined by the Herpin Index and the number of periods used for the multilayer. Figure 2 shows the passband transmission and the Herpin Index with the same design example of Figure 1. The transmission oscillates around the transmission of the uncoated substrate T_S and is enveloped by the transmission T_E of the equivalent layer itself. Within the passband there are again some characteristic points related to an edge filter. There is a so-called passband outset at λ_{outset} where $T(\lambda)$ equals T_S for the first time outside of the stopband; another point is at λ_{AR} where $T(\lambda)$ equals again T_S but in this case because the Herpin Index is unity; and there are two points at λ_{P1} and λ_{P2} where $T(\lambda)$ equals T_{Pass} marking the width of the required pass region.

Dependent on the actual requirements on an edge filter, five different spectral regions can be distinguished by the values of transmission and Herpin Index, respectively, shown in Table 1.

Table 1. Definition of filter regions of an edge filter in dependence on transmission and Herpin Index. AR stands for antireflection.

edge filter region	standard region	wavelength region	$T(\lambda)$	$E(\lambda)$ values
blocking	stopband	λ_{S1} to λ_{S2}	$< T_{\text{Stop}}$	imaginary
edge	stopband/passband	λ_{S1} to λ_{P1}	$T_{\text{Stop}} < T < T_{\text{Pass}}$	imaginary/real
ripple	passband	λ_{P1} to λ_{AR}	$\leq T_S$	$0 < E < 1$
AR	passband	λ_{AR} to $\lambda < \lambda_{P2}$	$\geq T_S$	$1 < E < n_S$
pass	passband	λ_{P1} to λ_{P2}	$\geq T_{\text{Pass}}$	$1 < E < n_S$ (nearly)

In contrast to previous definitions, in this definition of the different filter regions the edge of the stopband determined by the Herpin Index is within the actual edge region and not at the end of the stopband or at the start of the passband. Additionally and without any loss of generality, the required transmission within the passband is set as $T_{\text{Pass}} = T_S$ and the passband outset of the given multilayer marks the beginning of the pass region of the edge filter. These two definitions give the advantage to handle the blocking region and the edge region independent of the ripple region and the pass region. Blocking and edge slope are determined only by the refractive indices of the materials used and the number of periods, i.e. by the imaginary part of the equivalent index. Ripples and pass are determined by the real part of the equivalent index.

Now the slope of a steep-edge filter is defined by the spectral width of the edge region and the difference of the transmissions between blocking and pass, usually given in units of optical density. Thus, a state-of-the-art edge filter is characterized by 5 to 10 nm for the width and OD5 for the difference, for example. Choosing, for example, TiO_2 and SiO_2 with refractive indices of $n_A = 2.35$ and $n_B = 1.47$, resp., as suitable materials for an edge filter, an A/2 B A/2-trilayer with 40 periods and 81 layer, resp., meets such a slope. Besides the large number of layers there is no problem in general to fulfill actual requirements on blocking and edge slope by choosing suitable materials and the required number of periods. The AR region is automatically given by the corresponding wavelength dependence of the Herpin Index. So, the ripple region has to get most of the designer's attention.

3. STEEP-EDGE FILTER DESIGN WITH EQUIVALENT LAYERS

There is a straightforward solution to the ripple problem by applying a symmetrical trilayer as AR coating between the filter design and the ambient media, which was presented for the first time in 1966.⁵ Figure 3 shows the spectral performance within the edge region and the pass region of three long-wave pass designs according the known approach. These designs differ by different numbers of layers and, considering the presented definition of the edge region, they are shifted over the wavelength to get the same position of the passband outset. Because the Herpin Index is the same in each of the three designs, it is possible to apply also the same AR trilayer to each of the three designs. However, the more layers are used, the lower the influence of the chosen AR coating will be. But it is possible to change the optical thickness of the AR coating or to apply more than one AR coatings to improve the ripple performance.⁷

The AR trilayer used in Figure 3 is also a symmetrical A/2 B A/2 sequence and has a Herpin Index E_{AR} and a phase thickness Γ_{AR} . Applying this trilayer as AR coating to the standard long-wave pass design, described here as core stack with a Herpin Index E , the index condition $E_{AR} = \sqrt{n_s E}$ (if the AR coating is placed adjacent to the substrate) and $E_{AR} = \sqrt{n_s E}$ (if the AR coating is placed adjacent to the ambient medium) as well as the phase condition $\Gamma_{AR} = k\pi/2$ (with k an odd number) have to be fulfilled simultaneously. The refractive index condition can be fulfilled by shifting the optical thickness of the AR trilayer a little bit towards shorter wavelengths in comparison with the optical thickness of the core stack. The phase condition can be fulfilled by choosing a corresponding number of periods. Because per definition the edge region of the filter does not depend on the real part of the equivalent index, the equivalent index of the ripple region is always the same for all number of periods of the core stack. This means, in principle, the known solution given in 1966 with a period number of 12 should be also a possible solution for a period number of 40, for example. What has to be done is just a better adjustment of the AR trilayer to the actual core stack.

It is set as start design

$$\text{sub} / c_1(A/2 B A/2)^x (A/2 B A/2)^p c_2(A/2 B A/2)^y / \text{air}.$$

with $n_A = 2.35$ and $n_B = 1.47$. Sub and air stand for the substrate with $n_s = 1.52$ and the ambient medium with $n_0 = 1$. Two AR trilayers are placed between core stack and substrate, and core stack and ambient medium, respectively. The exponent of the core stack is used as parameter to meet an edge slope with a width of 5 to 6 nm at a difference of OD5 in transmission. The coefficients c_1 and c_2 for the QWOT as well as the exponents x and y are used as variables in an optimization procedure to get the most suitable adjustment of the Herpin Indices and phase thicknesses of the two AR trilayers to the given Herpin Index of the core stack. E and Γ are calculated for each of the trilayers but the optimization run is performed only within the defined ripple region from λ_{outset} to λ_{AR} .

The result of such an optimization does not cause a surprise for someone who is familiar with the theory of equivalent layers. The coefficients c_1 and c_2 do not change remarkably by changing the parameter p , the exponents simply increase with increasing p . One possible solution as final design is

$$\text{sub} / 0.956(A/2 B A/2)^4 (A/2 B A/2)^{40} 0.984(A/2 B A/2)^7 / \text{air}.$$

Figure 4 shows the transmission curves of core stack and final design within the pass region. The ripples are not disappeared but within the ripple region the average transmission is increased up to 95 %. Figure 5 shows the curves within the blocking region and Figure 6 gives a detail of Figure 5 within the edge region. The additional periods of the AR trilayers decrease T_{min} as expected, but they change neither the slope of the edge nor the width of the stopband. This effect results directly from the approach that the edge region is not connected with edges of the stopband of the core stack. However, smoothing the ripple region of a steep-edge filter causes the disadvantage of a significant increasing of the number of layers compared with the number of layers of the core stack used as start design.

Figure 7 shows the Herpin Indices of the different trilayers applied in the final design, in comparison with the required values according the AR index conditions. Within the ripple region given by the condition $0 < E < 1$, the required index values and the realized ones are in perfect agreement. Figure 8 shows the phase values of the two AR trilayers. In both of the used AR-trilayers, the AR phase condition is perfectly fulfilled close to the edge at 590 nm.

A usual thickness refinement is applied to this deduced steep-edge filter design by replacing the constant refractive indices with real ones and keeping the thicknesses of the core stack constant. Figure 9 shows the result of this procedure, with a further smoothing of the passband transmission, Figure 10 shows the thickness characteristic after the refinement, and Table 2 lists the layer sequence. There is a remarkable adjustment of all the layers of the additional AR trilayers. This effect gives a distinct indication for a further improving of the presented approach. Firstly, the periods of the added

AR trilayers can be optimized independently of each other, and secondly, even the layer thicknesses within the trilayers can be used as optimization variables. The latter method is also known by the theory of equivalent layers because the thickness variation within a trilayer change the possible Herpin Index within the range of the given values of the low and high refractive indices.^{8,9} However, this can be done easier by using the refinement procedure of any thin-film design software than by an explicit theoretical formalism.

Figure 11 shows an example of a measured transmission curve of a recently manufactured edge filter which was designed following the presented approach. The transmission within the blocking region is less than OD5 and the average transmission within the pass region is about 95 %. Passband outset is at 595 nm and the edge width down to the blocking value of OD5 is 6 nm. Finally, it has to be said, that all the definitions and derivations are not restricted to the given long-wave pass filter type and to the example positioned at an edge of about 595 nm.

4. CONCLUSIONS

Edge filters belong to those interference filters that are part of most optical arrangements, particularly of optical devices applied for fluorescence microscopy. State-of-the-art fluorescence detection requires steep-edges filters with spectral slopes of 5 to 10 nm for the transition region from blocking to the pass and with blocking values of at least OD5. Such requirements force the thin-film designer to work with a better definition of the edge slope of an edge filter. Accordingly, a detailed study of the different regions of an edge filter is presented and the following two essential conclusions can be drawn:

A) The transition region from blocking to pass is characterized by a wavelength point called passband outset where the transmission for the first time reaches its maximum outside the blocking region. This definition is independent of the respective pass type because only the direction of the transition changes if a long-wave pass or a short-wave pass is considered. The edge slope is then given by the spectral width from passband outset to that wavelength where the required optical density of the blocking region is reached for the first time.

B) This definition of the edge region provides the advantage of applying a simple standard thin-film design given by a symmetrical $(A/2 B A/2)^p$ multilayer as long-wave pass or short-wave pass, independently of the actual requirements. A multilayer like this can be described by the theory of equivalent layers with a Herpin Index and an equivalent phase thickness. Then, the imaginary part of the Herpin Index determines both the blocking and the edge region of the given multilayer, and the real part of the Herpin Index determines the pass region. The blocking behavior is determined only by the number of periods and the chosen refractive indices, and smoothing the passband is only a matter of a precise adjustment of the necessary AR coatings between the $(A/2 B A/2)^p$ multilayer and the ambient media.

It is shown that no further formalism than the theory of equivalent layers are required to realize a steep-edge filter design with 6 nm edge slope for the transition of 5 optical densities with an average transmission within the passband of 95 %. The presented filter design has 103 layers and is directly deduced from an edge filter design with 31 layers given in 1966. Applying a usual thickness refinement, further improvement of the spectral performance of the presented edge filter can be achieved. This result can be in fact explained by applying equivalent layers but it also initiates further investigations.

References

1. The Photonics Handbook™, © 2005 Laurin Publishing
2. A. V. Tikhonravov, M. K. Trubetskov, and G. W. DeBell, "Application of the needle optimization technique to the design of optical coatings," *Appl. Opt.* **35**, 5493-5508, 1996.
3. André Herpin, "Calcul du pouvoir réflecteur d'un système stratifié quelconque," *Comptes Rendus Academies des Science*, **225**, 182-183, (194).
4. L. I. Epstein, "The Design of Optical filters," *J. Opt. Soc. Am.* **42**, 806-810, 1952.
5. A. Thelen, "Equivalent layers in multilayer filters," *J. Opt. Soc. Am.* **56** 1533-1538, 1966.
6. A. Macleod, *Thin-film optical filters*, Third Edition, Institute of Physics Publishing, Bristol and Philadelphia, 2001.
7. Alfred Thelen, *Design of optical interference coatings*, McCraw-Hill, 1989.
8. P. H. Berning, "Use of Equivalent Films in the Design of Infrared Multilayer Antireflection Coatings," *J. Opt. Soc. Am.* **52**, 431-436, 1962.
9. M. C. Ohmer, "Design of three-layer equivalent films," *J. Opt. Soc. Am.* **68**, 137-139, 1978.

Figures

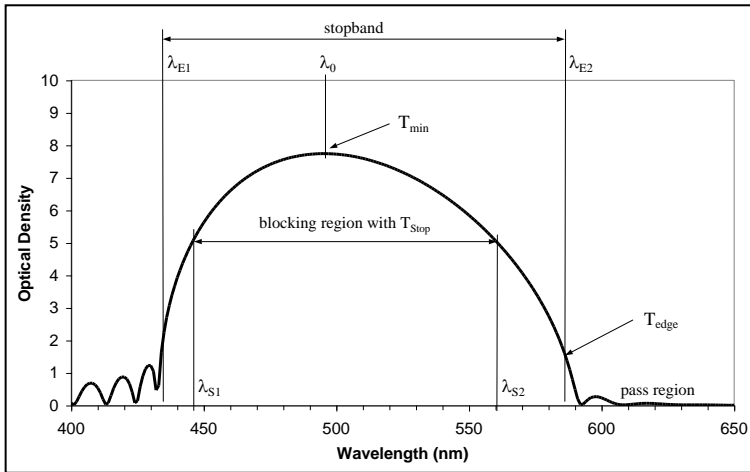


Fig. 1. Long-wave pass filter example with stopband and blocking regions (see text).

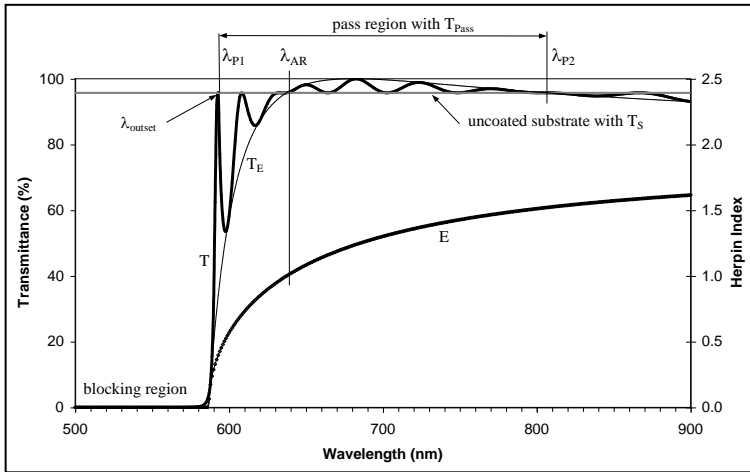


Fig. 2. Long-wave pass filter example with ripple and pass regions (see text).

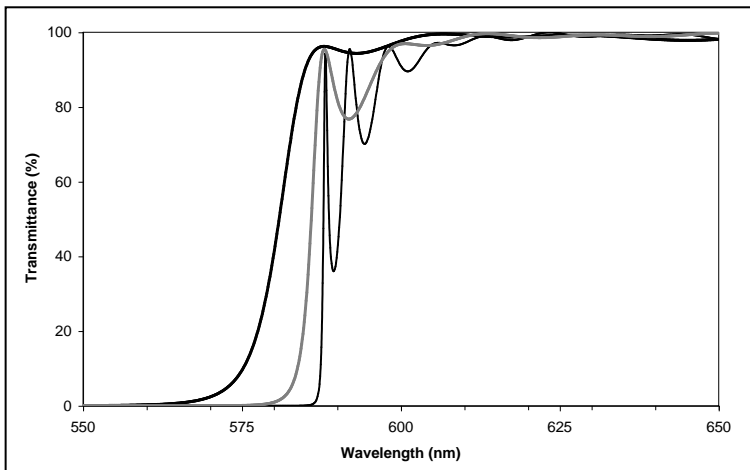


Fig. 3. Long-wave pass filters $n_S / 0.95(A/2 B A/2)^3 (A/2 B A/2)^p / n_0$, with $p=12$ and $\lambda_0=491.5\text{nm}$ (thick), $p=20$ and $\lambda_0=497\text{nm}$ (gray), and $p=40$ and $\lambda_0=500\text{nm}$ (thin), with $n_A=2.35$, $n_B=1.47$, $n_S=1.52$, $n_0=1$.

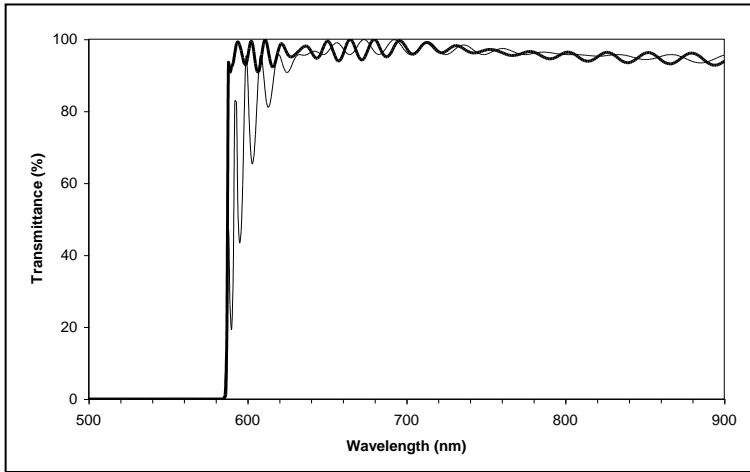


Fig. 4. Spectral performance of final design (thick) and core stack (thin) within the pass region (see text).

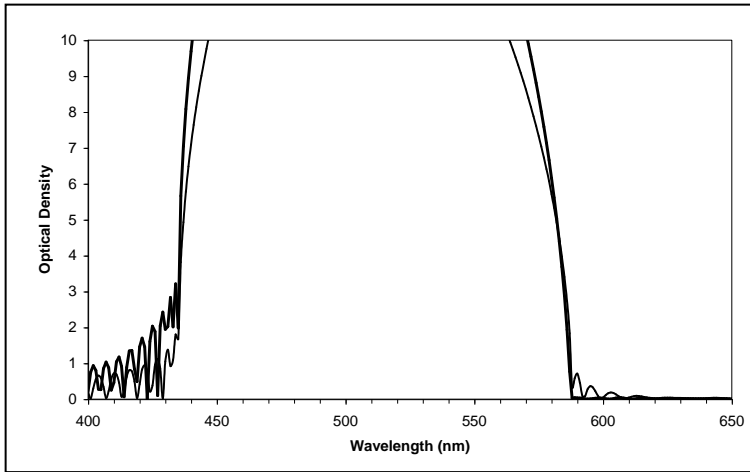


Fig. 5. Spectral performance of final design (thick) and core stack (thin) within the blocking region (see text).

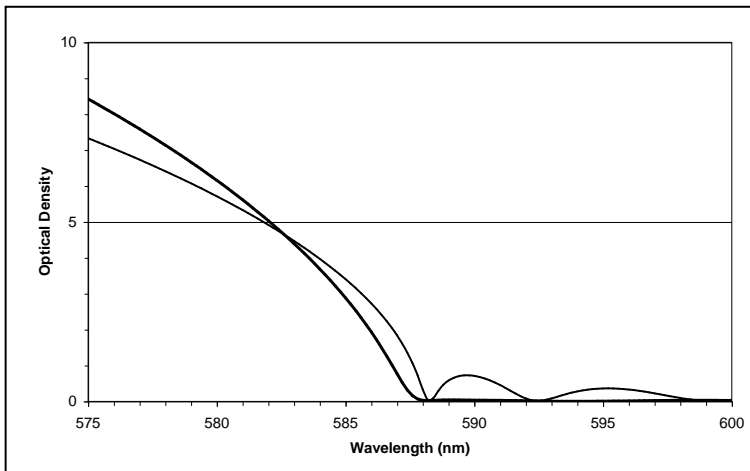


Fig. 6. Spectral performance of final design (thick) and core stack (thin) within the edge region (see text).

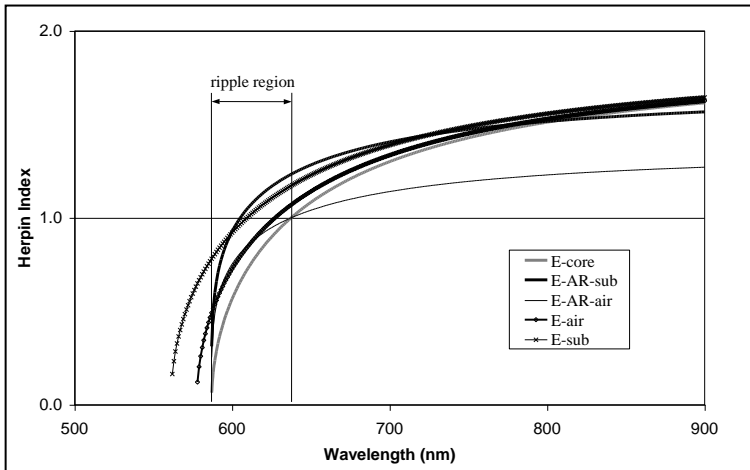


Fig. 7. Herpin Index plot of the AR trilayers E_{sub} and E_{air} of the final design, and the AR index conditions $E_{\text{AR-sub}}$ and $E_{\text{AR-air}}$ for the core stack (see text).

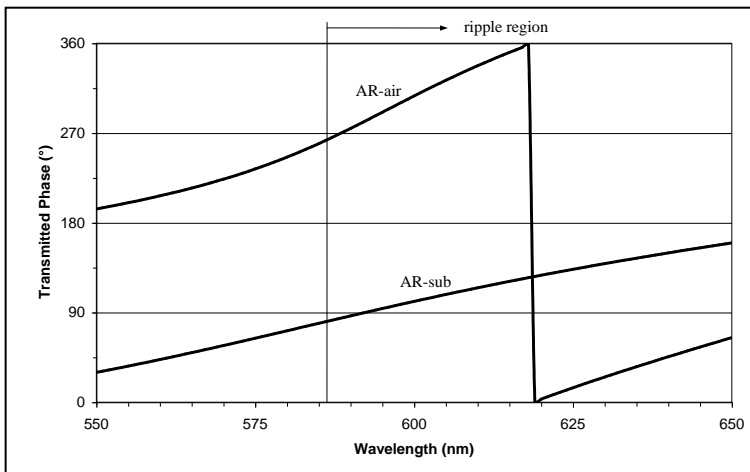


Fig. 8. Transmitted phase plot of the AR trilayers of the final design (see text).

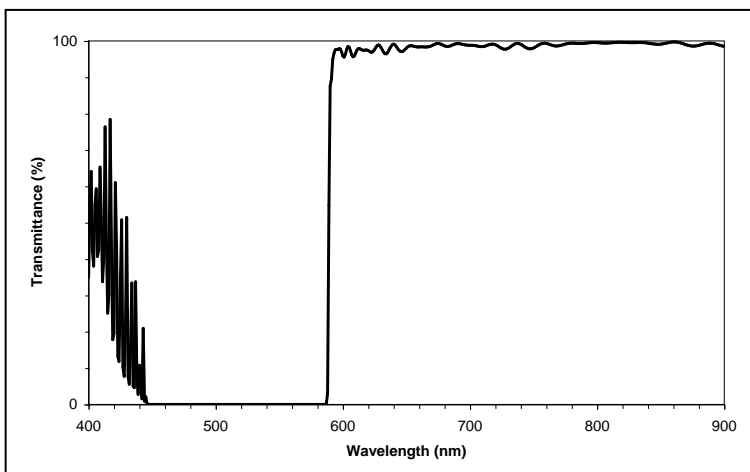


Fig. 9. Spectral performance of the refinement design with real refractive indices of TiO_2 and SiO_2 (see Table 2).

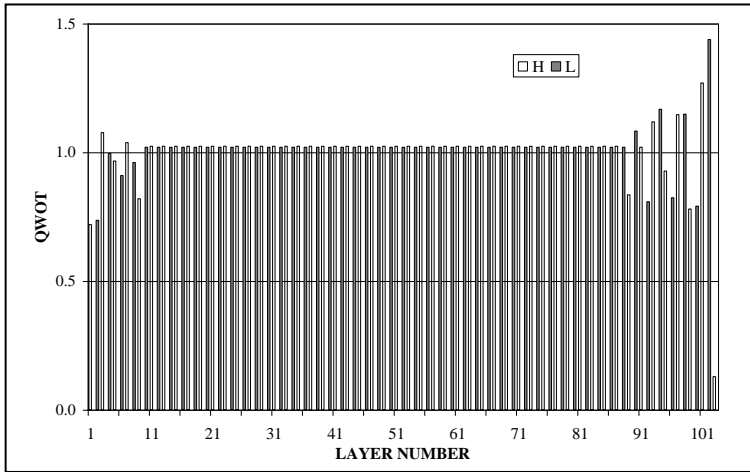


Fig. 10. Thickness characteristic of the refinement design (see Table 2).

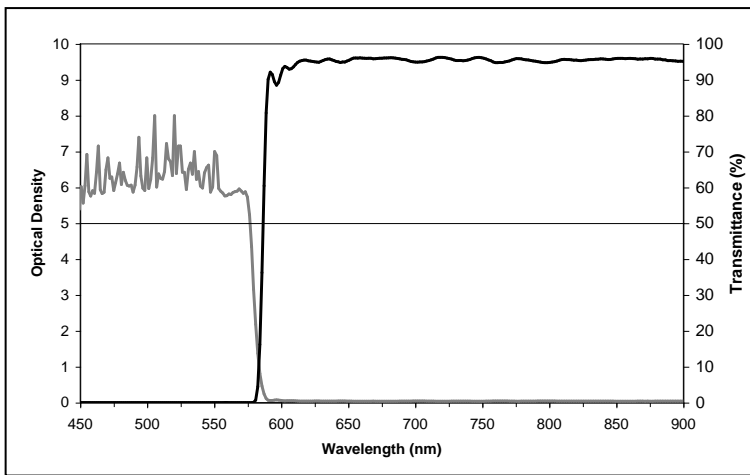


Fig. 11. Spectral characteristic of a long-wave pass filter LWP595 as example of a manufactured edge filter.

Table 2. Layer sequence of the refinement design, starting at the substrate. # is layer number, type is layer material, OT is QWOT at $\lambda_0=500$ nm, refractive indices according a quadratic wavelength dependence with $n_A(\lambda)=2.16+61354/\lambda^2$ and with $n_B(\lambda)=1.47+1087/\lambda^2$, $n_S=1.52$, $n=1$. Losses are negligible.

#	type	OT	#	type	QT	#	type	QT	#	type	QT	#	type	QT	#	type	QT	#	type	QT
1	A	0.719	17	A	1.024	33	A	1.024	49	A	1.024	65	A	1.024	81	A	1.024	97	A	1.146
2	B	0.736	18	B	1.020	34	B	1.020	50	B	1.020	66	B	1.020	82	B	1.020	98	B	1.148
3	A	1.076	19	A	1.024	35	A	1.024	51	A	1.024	67	A	1.024	83	A	1.024	99	A	0.779
4	B	0.995	20	B	1.020	36	B	1.020	52	B	1.020	68	B	1.020	84	B	1.020	100	B	0.791
5	A	0.966	21	A	1.024	37	A	1.024	53	A	1.024	69	A	1.024	85	A	1.024	101	A	1.269
6	B	0.909	22	B	1.020	38	B	1.020	54	B	1.020	70	B	1.020	86	B	1.020	102	B	1.438
7	A	1.037	23	A	1.024	39	A	1.024	55	A	1.024	71	A	1.024	87	A	1.024	103	A	0.128
8	B	1.190	24	B	1.020	40	B	1.020	56	B	1.020	72	B	1.020	88	B	1.020			
9	A	0.820	25	A	1.024	41	A	1.024	57	A	1.024	73	A	1.024	89	A	0.835			
10	B	1.020	26	B	1.020	42	B	1.020	58	B	1.020	74	B	1.020	90	B	1.257			
11	A	1.024	27	A	1.024	43	A	1.024	59	A	1.024	75	A	1.024	91	A	1.020			
12	B	1.020	28	B	1.020	44	B	1.020	60	B	1.020	76	B	1.020	92	B	0.808			
13	A	1.024	29	A	1.024	45	A	1.024	61	A	1.024	77	A	1.024	93	A	1.118			
14	B	1.020	30	B	1.020	46	B	1.020	62	B	1.020	78	B	1.020	94	B	1.167			
15	A	1.024	31	A	1.024	47	A	1.024	63	A	1.024	79	A	1.024	95	A	0.927			
16	B	1.020	32	B	1.020	48	B	1.020	64	B	1.020	80	B	1.020	96	B	0.823			